Evaluation of System Performance Phantom (SPP) for Image Quality Control in Ingenuity TF PET-CT Systems

HM Jamil[1], M A Rahman[2], Md Mubdiul Hasan[3]

[1]Secondery Standard Dosimetry Laboratory, INST, AERE, BAEC, Dhaka-1349, Bangladesh
[2]Health Physics & Radioactive Waste Management Unit, INST, AERE, BAEC, Dhaka-1349, Bangladesh
[3]Electronics Research and Development Department, Cleveen SC, 11120 Stockholm, Sweden

Abstract

Objectives: Clinical assessment: Radiologists utilize CT numbers to assess healthy and ill tissues; therefore, precision is essential. Most quality control protocols use different phantoms to check this crucial factor and other parameters. This study evaluates the performance of the System Performance Phantom (SPP) as it assesses all Image Quality Control parameters of a CT scanner (Part of TF PET-CT System, Ingenuity Model, Philips).

Method: At this cancer treatment center, quality control was carried out according to the factory IQ Check protocol, and advanced tests involved data acquisition at different collimations, kernels, slice widths, energy levels, and tube currents. We used system performance phantom during installation, which continued throughout the period. iPatient & CT viewer software of Philips on the console PC did data acquisition and image reconstruction and analysis. We retrieved the system's quality control reports from November 2017 to July 2020 and other raw data and examined them by MS Excel and Origin19b.

Results: After analyzing all reports, we got the mean CT number of 112.03 at a mean noise of 8.96 and a uniformity of 0.75618 (for the body section). The head section's mean CT number is 0.37 at a mean noise of 2.59 with a mean uniformity of 1.63. Moreover, the minimum pin diameter in the low contrast detectability test is 57% in 3.80-3.88mm at a 0.3% contrast level. The other parameters, slice thickness (50% FWHM) and spatial resolution (10% and 50% MTF), are compared with installation and present data. Finally, the linearity of CT number of different materials, and graphical presentation indicates very close values when compared with installation data.

Conclusion: The SPP is a valuable tool for ensuring image quality in Ingenuity TF PET-CT systems. Its application in three nuclear medicine centers in Bangladesh has improved confidence in the quality of PET-CT imaging services.

Keyword: Quality Assurance, CT Number, Spatial Resolution, Low Contrast Detectability, MTF

1. Introduction

The discovery of the X-ray by German physics professor Wilhelm Röntgen in 1895 sparked worldwide interest in the non-lethal use of radiation for medical imaging[1]. Over 75 years, this 2D X-ray technique has evolved into Computed Tomography, a more advanced X-ray imaging

capable of producing 3D body scans. Invented by physicist Allen Cormack and engineer Sir Hounsfield in the early 1970s, this machine was a significant technological advance in many respects [2][3][4][5]. 1971, the first patient brain scan was performed after EMI placed its first scanner at Atkinson Morley's Hospital in Wimbledon, England [5][6]. Spiral CT was launched in 1990 due to more ground-breaking advances in this field [7]. Ongoing refinement of CT imaging from axial to the helical, single detector to multidetector, X-ray tube up-gradation, and tube current modulation, as well as the computer system, are driving high-resolution diagnostic imaging at a minimum dose of radiation[8][9][10][11][12][13]. Besides this hardware advancement, it is quite reasonable to define the performance of the CT scanner in terms of image quality. We can investigate this image quality as the accuracy of reproducing the 3D attenuation map with the patient's correct geometry, and the reliability of this image is the assessment of the performance of a CT scanner[14][15][16]**.**

For safe clinical practice, either in diagnosis or treatment, the QC of the image is a crucial issue [17][18]. However, determining optimal image quality is a complex task involving quantitative and objective physical measures linked with subjective observer perceptions to indicate clinical performance [15]. This article concentrates on the physical aspect of CT image quality. Many agencies at the national and local levels provide guidelines for creating the best quality control program for CT facilities [19]. Some of the renowned bodies involved in setting X-ray equipment standards are the Association of Physicists in Medicine (AAPM), the International Commission on Radiation Units and Measurements (ICRU), and the ACR (American College of Radiology). The European Commission has advocated using image standards in European countries to assess image quality[20]. The Human Health Series, No.19 of IAEA, is another informative and complete guideline for quality control of CT imaging[21]. These guidelines include periodic tests to ensure accurate target and structure localization [22] as well as a complete evaluation of system performance and image quality[14][16][21][23][24].

Generally, most guidelines consider many factors in a CT examination that can affect the dose and image quality, collectively described by the image noise and spatial resolution. Changes to the scan's settings can regulate variables relating to the patient. However, most scanner settings are predetermined and do not allow users to change (e.g., detector array, materials, see Table-1). To define CT image quality, we can consider two categories of parameters- a. dose-dependent parameters and b. image processing and viewing parameters [20][25][26]. There is a wide range of tests and test tools for quality assurance. Usually, sophisticated tests are scheduled annually or for significant maintenance work[22][27]. A typical quality assurance program for the spiral CT scanner consists of testing: CT number, uniformity, image noise, contrast scale and mean (standard deviation), high-contrast resolution and low contrast resolution, laser light alignment and accuracy, slice thickness, artifacts, and patient dose [27][19][28][29]. International Electro-technical Commission recommends the expression of the quality of CT images in terms of objective physical tests, including- uniformity, linearity, and measures of the detective quantum efficiency of the imaging system using psychophysical evaluation[30]. For CT technology from installation to daily operation, IEC recommends IEC61223, “Evaluation and routine testing in medical imaging departments –Part 3–6: Constancy tests–X-ray equipment for computed tomography”[30]. This part covers all the variables interfering with the CT image quality and the methods of determining these variations. ICRU publishes many technical documents on CT performance evaluation, and Report 87 (2012) is a detailed one on CT image quality[31]. However, manufacturer's manuals

include standard tests and proper phantoms, which are undoubtedly the primary resources for quality assurance, and violations may cause warranty voiding.

Table-1: Factors Affecting CT Number

Factors Affecting CT Image	Protocol or scan parameter	Adjustable by the operator
	Equipment	Not adjustable, Equipment configuration set by manufacturer
	Image Analysis Condition	Adjustable by reporter
	Patient-related factors	Adjustable by technologist, nurse, doctor

Table-2: Adjustable Factors Affecting CT Number

Dose-related factor		**Image Processing factor**	**Operator**
Tube voltage (kVp)	Pitch	Reconstruction Algorithm	Experience
Tube Current (mAs)	Collimation	Filter/Carnel	Protocol Selection
Dose Modulation	Scan Mode	FOV	Multiple Scan
		Window level	

2. Defining the performance criteria of a CT Scanner in terms of Image Quality

2.1 CT number

There, we introduced a computed value Computed Tomography (CT) number, which determines the voxel value indicating the average attenuation of a given unit volume, and a computed tomography (CT) picture is nothing more than an attenuation map of an object reconstructed from the attenuation coefficient of the various materials making up the object. According to Beer-Lambert's Law for monochromatic X-ray passing through a homogenous material, the intensity reduction is expressed as a function of X-ray energy, path length, and material linear attenuation coefficient:

$$I = I_0 e x^{-\mu x} \ldots\ldots\ldots\ldots (1)$$

Where I_o and I stand for the initial and final X-ray intensity, μ denotes the material's linear attenuation coefficient, and x is the X-ray path length [32][33]. Rearranging the equation:

$$\mu = \ln\left(\frac{I}{I_0}\right)/x \ldots\ldots\ldots\ldots (2)$$

The equation becomes more complicated for multiple materials and polychromatic X-ray sources.

Similar to a bitmap picture, the intensity of a voxel (volumetric pixel rather than a regular pixel) can vary from 0% (total absence; black) to 100% (entire presence; white), with any fractional values shown on the screen in grayscale[34]. It is a relative measurement of the X-ray energy, which provides information about the tissue materials[32]. In the final image, radiopaque volumes of material with high attenuation have a white appearance on display, like bone, compared with the relatively darker appearance of muscle and fat as radiolucent volumes with low attenuation[35].

The CT number is expressed in the Hounsfield unit (named after Sir Godfrey Hounsfield) [15], and mathematically, the Hounsfield Unit of any given material is:

$$HU = 1000 \times \frac{\mu - \mu_{water}}{\mu_{water} - \mu_{air}} \ldots\ldots\ldots\ldots (3)$$

Where μ, μ_{water} and μ_{air} are, respectively, the linear attenuation coefficients of the material, water, and air [36][12][11]. Thus, one HU change represents a difference of 0.1% of the attenuation coefficient of water since the air's attenuation coefficient is nearly zero. Considering the radio-density of distilled water '0' (zero) while '-1000' of air at standard temperature (T= 0^0C) and pressure (P= 10^5 Pascals) using *Eq.-3*, a measurement system developed to define the CT image known as the Hounsfield scale[21]. In the first scanner, Sir Godfrey Hounsfield used the scale -500 to +500HU to create the CT image [2]. CT scanners in medical practice can present HU within a range of –1024 HU to +3071 HU[37], where the cancellous bone is +700HU, and the dense bone is +3000HU[38]. However, whatever the scale is ±3000 or ±1000 or ±500 HU in a grayscale image, the voxel will take any value between 0 and 255. Figure-1 represents a typical Hounsfield scale.

The reliability of CT numbers is crucial as several studies warned that it varies from machine to machine; even the same patient with different scan volumes shows deviation[39][40]. So, the reliability of CT images depends entirely on the reproducibility of CT numbers during calibration. Most phantoms used water or water-equivalent material to calibrate the CT scanner, and the CT number of water is considerable at 0HU. In the system performance phantom, we have two sections: the head section (field with water, 0±4 HU) and the body section (nylon, 102±18 HU) [41]. So, measuring the CT number of these two sections provides the mean CT number of the uniform layer. The size of the ROI is a critical factor. The region of interest (ROI) for CT number evaluation is 5024±500mm^2 area for head phantom and 11300±1000mm^2 for body phantom[41]. The recommended ROI for CT number measurement is 10% of the diameter of the image of the phantom [42].

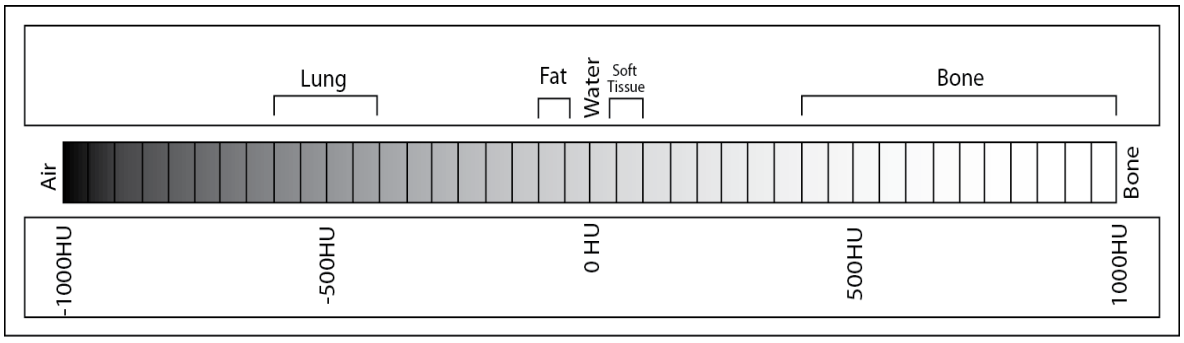

Figure-1: Hounsfield scale

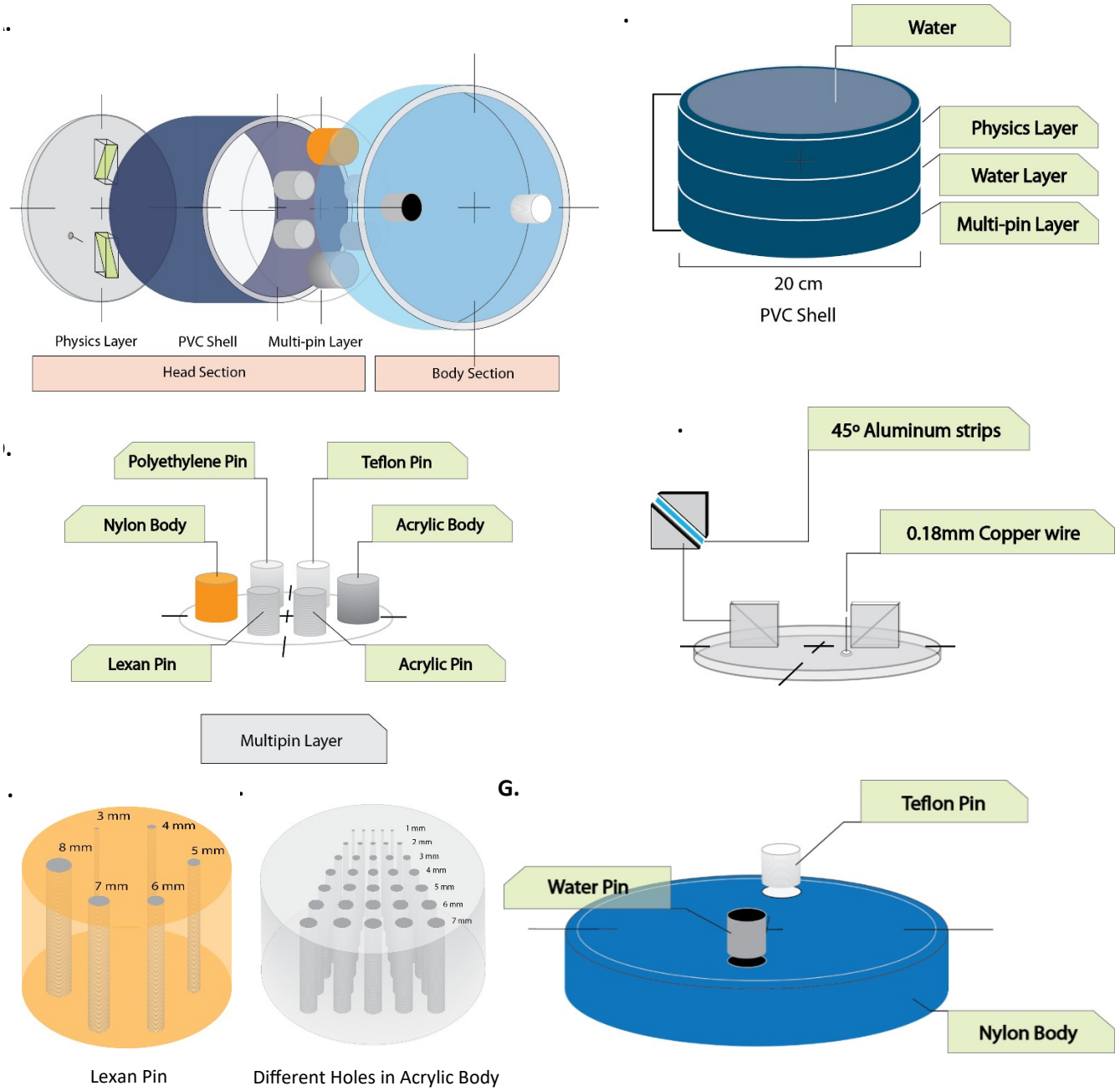

Figure-2: **System Performance Phantom (A**); two portions of this phantom-Head Section and the Body Section exist. **Head section (B):** The head section (Diameter =200 mm) is made of a Polyvinyl chloride (PVC) shell, which is filled with water. It consists of three layers. **Physical layer(C.):** This layer consists of Aluminum strips embedded at 45 degrees and a 0.18 mm copper wire used in resolution test and tomographic section thickness (slice width) measurements. **Water layer**: This layer is used to measure noise and uniformity. **Multi-pin layer (D.):** This layer checks the contrast scale. This layer contains various pins of materials, such as Lexan, Acrylic, Teflon, and Polyethylene. There is a **Nylon** (Aculon) **body** (**E.**) with six smaller Lexan pins (of different diameters- 3, 4, 5, 6, 7, and 8mm, respectively) and an **Acrylic body (F)** with seven rows of holes of different diameters. Each row has five

equidistance holes of the same diameter (**Row 1:** 1.00 mm holes, 2.00 mm apart; **Row 2:** 1.25 mm holes, 2.50 mm apart; **Row 3:** 1.50 mm holes, 3.00 mm apart; **Row 4:** 1.75 mm holes, 3.50 mm apart; **Row 5:** 2.00 mm holes, 4.00 mm apart; **Row 6:** 2.50 mm holes, 5.00 mm apart; **Row 7:** 3.00 mm holes, 6.00 mm apart.). **Body section (G.):** The phantom body consists of a nylon cylinder. It is 300 mm in diameter. The body phantom has two features: Teflon and Water (phantom liquid) pin.

2.2 Noise

Considering a uniform material layer, in a perfect world, the HU of a uniform object will always be the same; for example, the HU of water is zero, but in reality, in a CT image, the CT number is around a mean value. We consider this deviation from the mean value as noise. So, measuring the CT number of uniform water and nylon provides the mean CT number, where the standard deviation is the estimated noise of the uniform layer[21][34]. A typical range of noise for a spiral CT scanner is ±4 HU(for water) [43]. The possible noise sources are Quantum noise, Electronic noise, and noise due to the reconstruction algorithm, e.g., back-projection. However, photon flux is one behind the noise in the final image. The number of photons on the predicted beam is not equal when crossing any cross-sectional body region; the relationship is inversely proportional (Eq.-4).

$$Noise\,(Standard\ deviation) \propto \frac{1}{\sqrt{no\ of\ Photons}} \quad \ldots\ldots\ldots\ldots\ldots\ldots (4)$$

The operator adjusts other factors, such as scanning time and slice thickness, to reduce the noise level in the reconstructed image.

2.3 Uniformity

During CT, when the X-ray tube rotates around a uniform object (cylindrical shape) positioned at the center of the bore, the beam's length through the object and the density of the material are always the same. That is why, for a uniform object, the uniformity of the CT number specifies that the calculation of the CT number does not shift concerning the location of the chosen ROI or the phantom position relative to the isocenter of the scanner. We measure the uniformity by placing four additional regions of interest (N, E, S, and W) near the edge of the image of a uniform head and body section of the phantom **(Figure-3)**. Recommended diameters for the body and the head layer are 30-32cm and 15-21cm, respectively[21]. It can be valuable to check CT number uniformity for large fields of view. Considering a breast cancer patient is undergoing radiotherapy during CT simulation, the target organ breast is at the periphery of the scan area. So, this parameter ensures reliability between the center and edges. There is no universally accepted value for uniformity; however, a modern scanner allows ±5 HU at room temperature and pressure. The permissible value in Philips protocol is ±4 HU for water (head section) and ±8 HU for nylon (body section)[41]. IAEA documented tolerance limit for uniformity is ±10 HU.

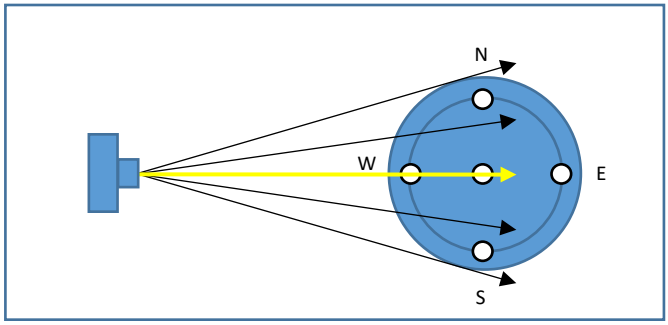

Figure-3: In any direction through the center attenuation is highest then others and, the path length is longest (yellow line).

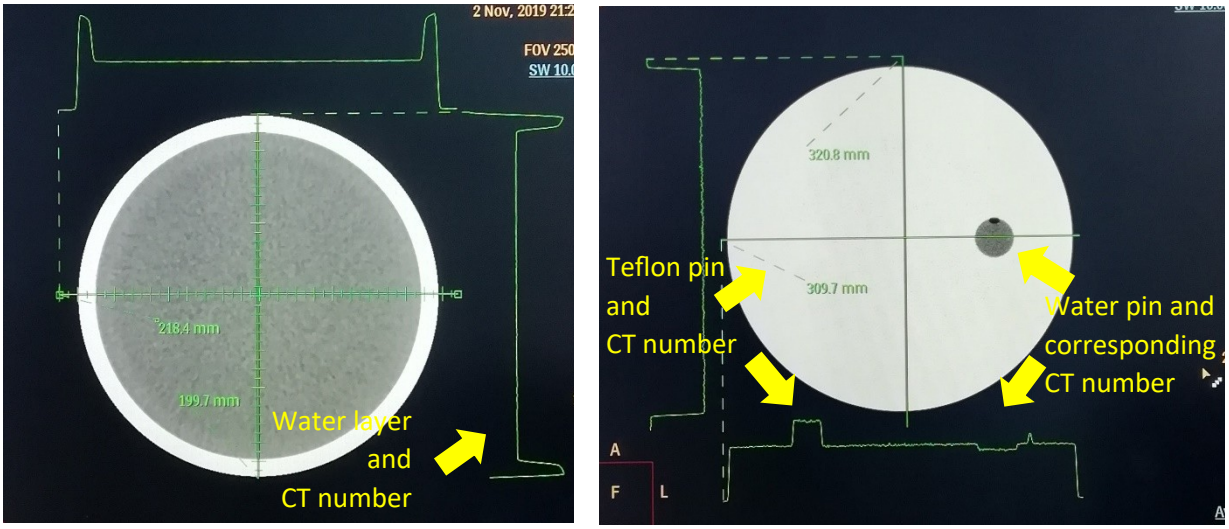

Figure-4: CT number profile of (a) Head water layer; (b) Body (Nylon) Teflon pin is not visible at W=500 and L=200.

2.4 Linearity

In several studies, linearity in CT numbers is considered the range of CT values for a given material that stays relatively constant across time [44]. In the system performance phantom, the Multi-pin layer (**Figure-2-D**) contains four pins of different materials, Lexan, Acrylic, Teflon, and Polyethylene, with HU, ranging from approximately -1000HU to +1000HU (**Figure-5 & 13**) [41]. We checked the CT numbers linearity for these materials against threshold energies at 120 kVp, 450mAs. The minimum area should be 200±15 mm^2. Commissioning tests need to use the same phantom available for subsequent routine QC. In addition, we employed a CIRS Model 002LFC, CIRS, USA, IMRT Thorax Phantom to test the linearity of CT numbers in tissue equivalent materials [45]. According to ICRU, Tissue equivalent materials or tissue substitutes are a substitute for original human tissue and organs for a given radiation type and energy by absorbing and scattering the radiation to the same extent as actual tissues within known and acceptable limits[21][44][46]. This study compares the CT numbers of different materials with previous data. The scan protocol was- Thorax (10-30kg), Axial mode, High Resolution, 120kV, 330mA, Filter

YC. All measurements were performed by positioning a small ROI well within each of the checked pins and regions (Area 200±15 mm^2)[41].

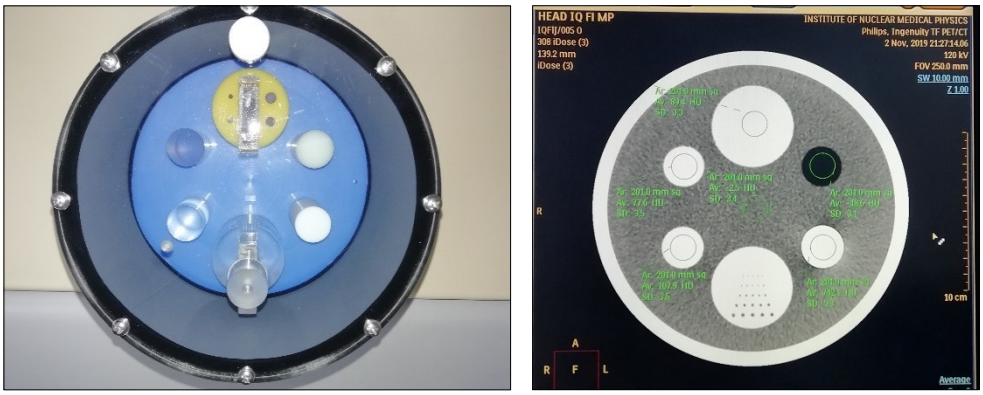

Figure-5: Different materials of System Performance Phantom

2.5 Low contrast performance

Noise is one of the main reasons for the poor image of low-contrast tissue. A common approach is increasing tube-current-time products, which may reduce noise but contribute some extra dose to the patient[47]. Several studies suggested the interference of modern reconstruction algorithms (iterative reconstruction) with low contrast detectability and dose reduction[48][49][50][51]. In specification literature, low contrast detectability is often cited as the smallest noticeable object for a given dose at a given contrast[21]. Since this measurement is directly related to the image's output, it is a significant parameter for acceptance verification[52]. It specifies the contrast information that can be visibly replicated when there is a slight change in density compared to the surrounding area, ensuring that more subtle objects can be seen in the image[53]. This is particularly important when attempting to classify tumors of low density that lie in soft tissues. The brain, kidney, and liver are the most common places where this is important[49][54] [55]. This test checks the capacity of the scanners to detect items that differ only marginally from their context (<10%). Different phantoms use different arrangements for this test[54]. In CatPhan600, there are five acrylic spheres with a 30mm diameter circular pattern (Diameter, D=2,4,6,8,&10mm) for low contrast detectability test[19][53].

On the other hand, in the GE phantom, there are four holes on a rectangular plastic slide or PMMA for LCD measurement[56]. However, in system performance, phantom six smaller Lexan pins of different diameters 3, 4, 5, 6, 7, and 8mm are clockwise oriented in a body made of Nylon (Aculon). Such a module is challenging to identify with the naked eye. Philips's algorithm integrated with the IQ Check protocol automatically measures the low contrast detectability using the multi-pin layer Fig-4(E) that the minimum pin diameter (in mm) detected at 0.3% contrast[41].

2.6 Slice thickness measurement

When discussing a Computed Tomography (CT) scanner, the term slice thickness describes the thickness of each image slice. Collimators in a CT scanner are responsible for controlling the projection of the X-ray beam and, hence, the thickness of the slices that will be exposed for data

collection. Different CT scanners and imaging protocols can result in different slice thicknesses. Like most things, the X-ray intensity is highest in the middle and decreases as you move outward. High dosage in the overlapped area or data loss from insufficient photons at the edge are the two main consequences of this fault in beam collimation. Therefore, the slice thickness test guarantees the correctness of the collimation. Full-width at half-maximum (FWHM) is the unit of measure for this parameter (AAPM Reports No. 1 and No. 28)[57]. Multiple modules can be combined with a phantom to evaluate slice thickness, and there is also a phantom available separately for testing image quality. This test is commonly implemented with a module consisting of crossed high signal ramps at a fixed angle[53][58]. For this test, the CT number profile of the wire is evaluated, and the CTMax is determined to compute FWHM[53] using the CatPhan 600's two pairs of 230 wire ramps. Two tungsten carbide beads, each 0.28-millimeter diameter, are utilized to gauge slice thickness in the ACR Accreditation Phantom (Model 646, Gammex). One such option is to use a tungsten disc 1mm in diameter and 0.05mm thick, placed in a plastic tube 4cm in diameter that is tissue equivalent[59].

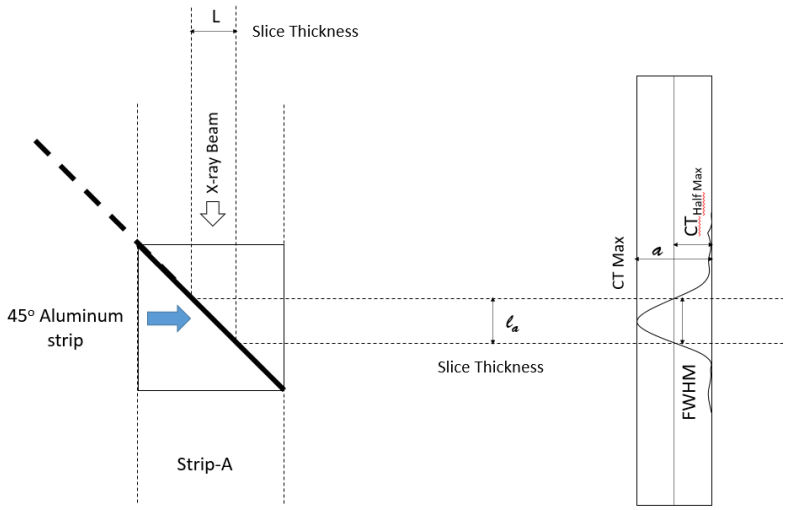

Figure-6: Schematic diagram showing the beam width and slice thickness across the slice plane.

In the system performance phantom in the head section, a thin sheet of Aluminum inclined at 45° is used to measure slice sensitivity profiles (SSP)[41]. The IQ software automatically calculates the slice thickness and shows the result for different pitches and collimation. The maximum tolerance limit of deviation for different slice thicknesses is different for each thickness (Thickness 2 mm: ±1 mm; Thickness >1 to <2 mm: ± 50%, and thickness < 1 mm: ± 0.5 mm). The 0.625 mm and 1.25 mm results appear wider due to the image's limited resolution and the measuring ramp's thickness [41]. Slice thickness is typically between 0.5mm and several millimeters. Higher resolution can be achieved with thinner images, but this comes at the cost of potentially longer scan time and increased radiation exposure to the patient. A thicker image can be acquired rapidly and with less radiation exposure; however, the resulting image may lack details. For instance, thinner slices may be preferred when imaging minor anatomical structures or lesions, but thicker slices may be more appropriate when screening or monitoring more significant anatomical regions.

2.7 Spatial resolution

Spatial resolution measures a scanner's ability to discern how accurately two similar objects of very high contrast and small size can be distinguished. Generally, a bar phantom of a set of holes or bars and spaces of constant equal dimension is a standard phantom to measure spatial resolution[53][60] [61]. The smallest row, where all bars and spaces can be seen clearly (Fig.-6), has better scanner output and image quality. Each bar plus adjacent space constitutes a line pair. Bar patterns generally represent a spatial frequency in line pairs per millimeter (or centimeter) rather than specifying bar width[53]. The following equation defines spatial frequency:

$$Spatial\ frequency = 1/(\bar{width} + hole\ width)$$

where bar width and *hole width* are in millimeters. Manufacturers choose less attenuating materials like acrylic or low-dense plastic and holes filled with water or air (CatPhan, GE CT Phantom) [14] [56]. In ACR, phantom line pair materials are Aluminum and polystyrene[61]. Physical observation of these bar patterns is an easy and straightforward approach to measuring spatial resolution[14]. However, the spatial resolution test is done by automated software provided by the manufacturer in terms of the modulation transfer function(MTF), the most common tool to determine the spatial resolution of CT, optical X-ray, and film X-ray systems using Fourier transformed the line spread function (LSF), point spread function (PSF), or edge spread function (ESF)[62][63]. Scanned objects have values between 0 and 1; however, the closer to 1 an object is, the better the MTF of the scanner. An MTF value of 0 would mean the image is blank and contains no information about the object scanned[18][64]. This study measured the spatial resolution with MTF of a 0.18mm copper wire of the phantom's physics layer by an impulse response program integrated with constancy test protocol[41].

2.8 Quality Control Phantom

During the last century, CT's development was immediately followed by modifying previous quality control tools and adding a new one as the application of CT spread to new areas of the imaging field like 4DCT, cone-beam CT, and dedicated CT for breast [28][57]. Dose constraints and limits on x-ray tube output and detector efficiency cause statistical uncertainties in attenuation measurements [57][65]. Ensuring radiation safety without compromising image quality drives the development of the latest image quality phantom. Quality control phantoms for testing different image quality parameters in computed Tomography (CT) are commercially available[19]. Old phantom technology ignored the geometric features of the CT as well as the physical parameters (e.g., kVp, mAs, rotation angle). American Association of Physicists in Medicine, Taskforce on CT scanner phantom, introduces the AAPM CT Test phantom, widely used in acceptance testing and quality control programs [47]. The CIRS AAPM CT Performance Phantom (Model 610) provides the user with a unified test object for the measurement of ten different CT performance parameters (Noise, Sensitivity, Mechanical Alignment, Beam Hardening, Slice Thickness, Size Independence, Radiation Dose, Spatial Uniformity, HU Linearity, Spatial Resolution)[66]. The phantom design is based on the guidelines presented in Report #1 of the American Association of Physicists in Medicine Task Force on CT Scanner Phantoms[57]. Sun Nuclear Corporation offers CT ACR 464 Phantom for multi-modality CT accreditation with four modules for CT number accuracy, Slice thickness, Low contrast detectability, uniformity, and Spatial resolution measurement[59][61]. The Phantom Laboratory, another company, has manufactured dependable, high-precision phantoms and innovative custom solutions for medical imaging and radiation therapy since 1989. Their Catphan series 500 or 600 are top-rated worldwide [19]. The Catphan®

600 comprises five modules enclosed in a 20cm housing- a. Slice Geometry and Sensitometry Module, b. Bead Geometry Module, c. High-Resolution Module, d. Low Contrast Module, e. Uniformity Module[67]. This study's main objective is to define a CT scanner's performance by applying a manufacturer-recommended phantom, evaluating image quality, and checking the positions of variables in the reference range.

3. Materials and method

Regarding image quality, we have measured a CT scanner's performance integrated with the Ingenuity TF PET/CT System, Philips. This 128-slice CT scanner has an 80 kW X-ray generator with four 80, 100, 120, and 140 kVp energy available for the scan. The stable state detector system is GOS with 40mm in width. We installed this scanner at the Institute of Nuclear Medical Physics in 2017 and performed all the quality control procedures according to the manufacturer **(Table-3)**. For the period 2017 to 2020, we have analyzed the IQ Check and constancy test data available. These protocols involved data acquisition at different collimations, kernels, slice widths, energy levels, and tube currents. We used system performance phantom during installation, which continued throughout the period. This phantom is a Philips product commonly used to check the image quality of the CT machine. Short tube conditioning stabilizes the X-ray tube's temperature during the scan and removes any moisture in the tube environment. We regularly did air calibration before the IQ check to remove any artifacts in the image. iPatient and other integrated applications of Philips on the console PC did data acquisition and image reconstruction. For visual review and analysis, we utilized Philips' CT viewer software. We retrieved the system's quality control reports and other raw data and examined them by MS Excel and Origin19b. We set our MS Excel template to draw the normal distribution curve and fit our data to check each parameter's distribution around their mean values in the reporting period. **Figures 8, 9, and 10** offer average values, maximum variance from average values, the absolute difference between the minimum and maximum values (range), and standard deviations (SD) of calculated CT numbers for each parameter.

Table 3: Quality Assurance of Ingenuity CT Scanner Philips at INMP

	Test Name	**Frequency**	**Objective**
1.	Short Tube Conditioning	Frequently	Tube heat stabilization
2.	Long Tube Conditioning	If necessary	Installation, Accessories replacement (ex., X-ray tube), Artifacts
3.	Air Calibration	Weekly	Artifacts
4.	IQ Check	Weekly	Image quality (Head Section)
5.	Monthly IQ Check	Monthly	Imager quality (Head and Body section)
6.	Constancy Test	Monthly	Advance Test (Detailed), Installation, Accessories Replacement
7.	Temperature Stabilization	If necessary	Optimum X-ray Tube performance

4. Result and discussion

4.1 Consistency of CT number, Noise level, and Uniformity

We present the CT number, noise, and uniformity of the system performance phantom's head section and body section graphically in **Figures-7** and **8**, respectively, from 2017 to 2020. The mean CT number is -0.37 and 112.0 for the head and body sections, respectively, where the tolerance limit is -4 to 4 and 103.4 to 115.4[21][41][46]. In the distribution curve, 61.8% of head CT numbers cover $1^{st}\sigma$; however, 66.29% of values of the body CT number are in $1^{st}\sigma$. The following parameter, noise, is a critical limiting factor in CT since much soft tissue detail is low contrast in nature[65][68][69]. Its effect on the image is to place a lower limit on the level of subject contrast, distinguished by the observer[68]. As the calculation aims to calculate the CT number within noise limits correctly, the line graph **(Figure-8)** shows that the mean noise level is 2.59 in the head section, where 83.14% of values cover $1^{st}\sigma$ (2.59 to 2.63). The body section noise level is 8.959 (mean), where most (52.81%) of the values lie in $1^{st}\sigma$ (8.83 to 9.09). All the values are within the tolerance range of 2.3 to 3.1 (head) and -8 to 8 (body) for the reporting period[21] [46][60][70].

The percentage of noise is calculated as

$$Noise_{percent} = \{SD /(Average\ CT\ Number + 1000)\}x100$$

During the reporting period, the percentage of noise was from 0.24% to 0.27% in the head section and 0.78% to 0.83% in the body section. In Philips protocol, the acceptable maximum noise level is 10%[41] or, according to Report No. 19 ±25% of the baseline value [21].

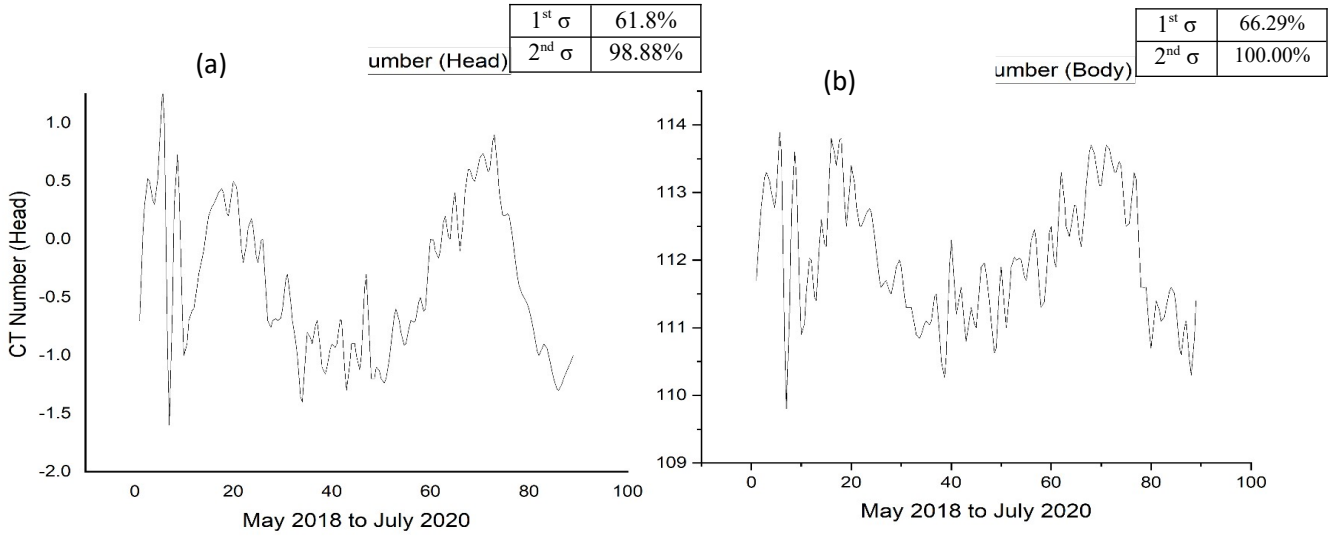

Figure-7: CT number of Head (a) and Body (b) section of the system performance Phantom for the period of May 2018 to July 2020.

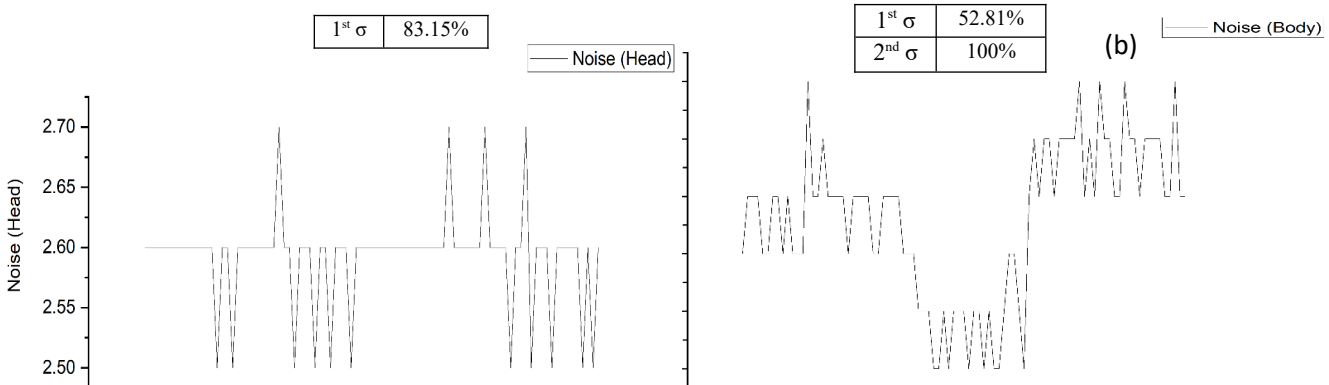

Figure-8: Noise of Head (a) and Body (b) section of the system performance Phantom for the period of May 2018 to July 2020.

The uniformity test ensures the reliability of CT numbers in the treatment area. Before, the measurement scanned image was checked slice by slice through the head and body section, as artifacts contribute to variation in CT number and noise. In the present study, the mean uniformity is -1.63HU in the head section for the uniform water layer, and in the body section, it is 0.76 HU **(Figure-9a & 9b)**. Here, the uniformity distribution shows that 48.31% score is within -1.63 to -1.79 HU ($1^{st}\sigma$) for the head section, and 54% score is within 0.76 to 1.39 HU ($1^{st}\sigma$) for the body section. There is no universally accepted value for uniformity; however, a modern scanner allows ±5 HU at room temperature and pressure. The permissible value in the Philips protocol is ±4 HU for water (head section) and ±8 HU for nylon (body section) [37], whereas the IAEA protocol accepts up to ±10HU variation [17].

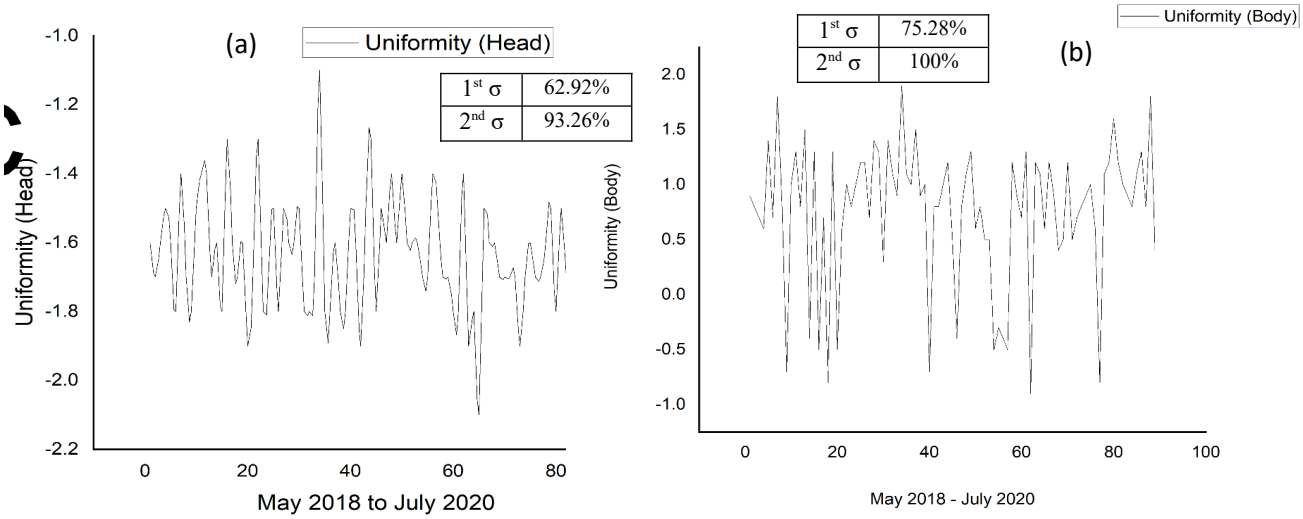

Figure-9: Uniformity of Head (a) and Body (b) section of the system performance Phantom for the period of May 2018 to July 2020.

The Philips IQ check protocol automatically aligns the Phantom (SPP) at the center of the bore, which is also crucial. Due to deviation from the center point, the distance from the X-ray tube varies, particularly during uniformity check, and the central ROI may mislead the result. It is also conducive to using integrated QC software capable of reproducing ROI of the same diameter at the exact location for time-to-time measurement.

4.2 Resolution and Contrast Performance

The concepts of resolution and contrast are frequently confused and incorrectly interchanged. It is expected that a high-resolution image will be more informative and detailed. Here, LCD defines

the detectability of low-density tissues in the low background, and spatial resolution is the ability of a scanner to differentiate objects depending on two spatial dimensions of an image length and width[52].

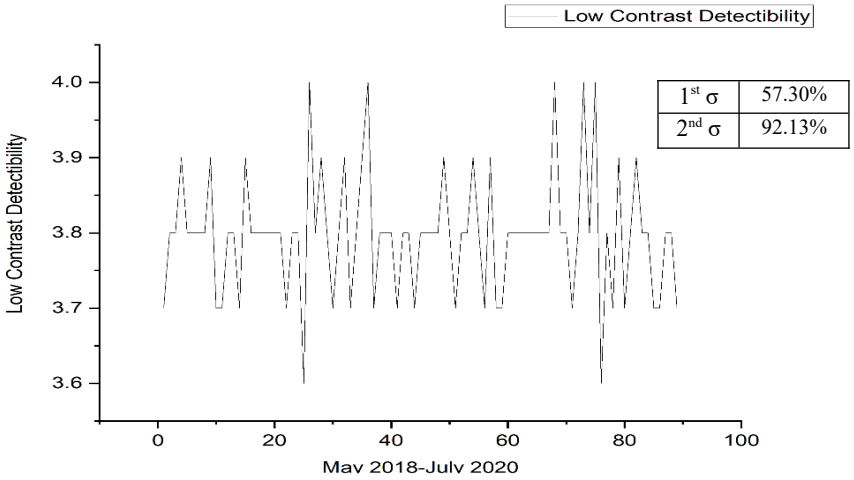

Figure-10: Low contrast detectability of the system performance Phantom for the period of May 2018 to July 2020.

The low contrast resolution or detectability performance of this CT scanner is excellent as the minimum pin diameter detected by the system is 3.80 mm (mean), where the reference limit is 3 to 5mm at 0.3% (3HU) contrast level[41]. Low contrast performance is probably the most significant performance test for quality management[71]. It ensures the detection of tissues with very close density. Throughout the reporting period, 57.30% of the LCD level is between 3.8 to 3.88mm. However, LCD depends on the observer's visual ability, and contrast to noise ratio dictates the result[72]. For this scanner, the spatial resolution was determined by MTF at 10% and 50% levels compared with installation data and graphically presented in Fig.7. In the line graph; there is no significant deviation of MTF (10%) values for collimation 64x0.625, 40x0.625, 20x0.625 and 32x1.25 from previous values (Blue line). However, for the 40x0.625 and 20x0.625 collimation, the MTF (50%) value is slightly different from the previous position, but the others are the same. SR should be routinely monitored for CT; however, the calculation of the MTF during routine QC tests is too complicated; therefore, an alternative estimate of SR is obtained using visual inspection of bar patterns **(Figure-12)** [53][73].

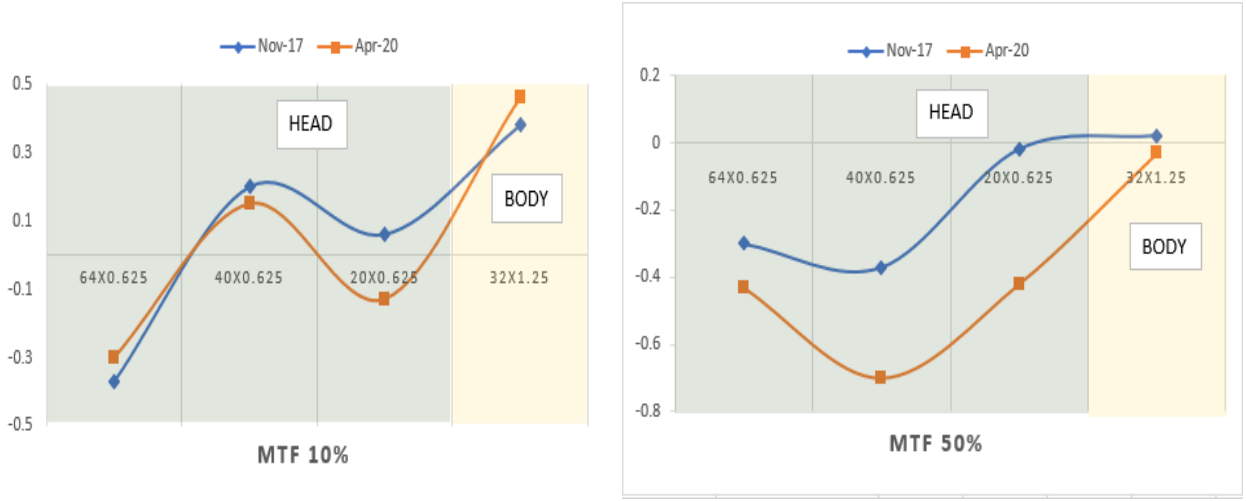

Figure-11: Spatial resolution: MTF 10%(a) and 50%(b) for different collimation settings in 2017 and 2020.

In Figure-12, the smallest objects are visible in the 5th line, and the corresponding spatial frequency is 0.22 lp/mm. Due to the relatively simple and fast calculation methods, the qualitative use of bar patterns to determine spatial resolution has acquired widespread use and remains standard clinical practice. Identifying structural edges, tumor margins, tiny foreign bodies, and tiny bony structures is necessary. However, the spatial resolution depends on several factors – reconstruction matrix, detector width, slice thickness, object-to-detector distance, FOV, focal spot, and matrix size.

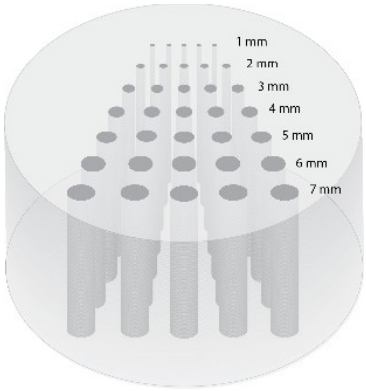

Figure-12: Different Holes in Acrylic Body for spatial resolution assessment

We assayed the linearity of the CT number of different materials using two different phantom-system performance phantom (SPP)[41] and Thorax phantom(CIRS)[45]. The linearity of the CT number of other materials in the multi-pin layer of SPP is presented in a line graph (Fig.8) and compared with the standard. Ideally, the CT number of tissue-equivalent materials at standard protocol should be the same over time. The deviation from previous data is insignificant, except the Teflon shows approximately a 100HU difference from the standard value at SD±20.98HU. In the second Phantom, IMRT Thorax phantom, the mean CT number of the water equivalent insert was -14.3 HU in November 2019, which was -15.1 HU in May 2018. The mean CT number for bone materials is 835.6HU (SD±47.6); the previous reading was 833.6HU (SD±58.5). The lung inserts also scored a very close CT number to the previous value. The graphical presentation is given in Figure 10 (c). In practical applications, quantifying radio density, according to the Hounsfield Scale, is the principle of CT imaging, and such a modality, when used in dose calculation for radiotherapy, becomes more critical. At this center, the reproducibility of the CT number for different materials is within acceptable limits.

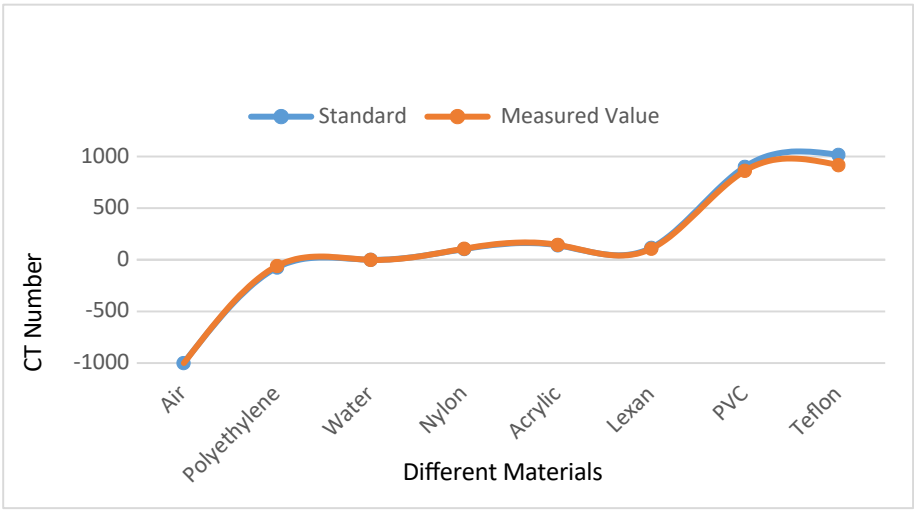

Figure-13: CT Number Linearity of Different Materials of System Performance Phantom with standard value.

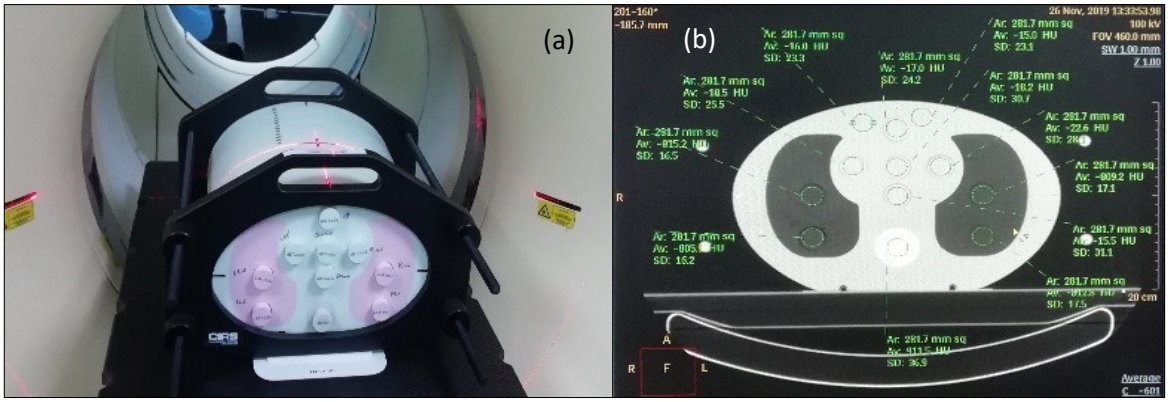

Figure-14: a. IMRT Thorax Phantom; b. CT Number of different rod inserts at 100 kV, 333mAs, SW=1.25mm, FOV=481mm;

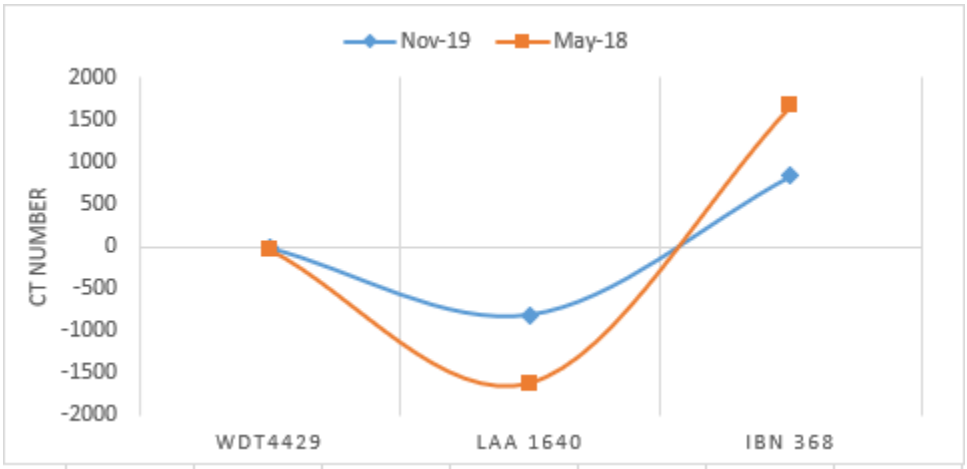

Figure-15: Comparison of CT Number of different materials IMRT Thorax Phantom; at 2018 and 2020.

Slice thickness

The result of slice thickness is given at 50% FWHM and presented in Fig-8. We checked slice thickness at different pitches and collimation (See Table-4) and cross-matched to see whether the measured values were within the tolerance level. The scan was in 2D mode at 120kVp, 200mAs, FOV 250, with a scan time of 0.75s, 768 X 768 matrix. We plotted the values of two data series of November 2017 and July 2020 for ten sets of parameters in a line graph **(Figure-16)**. There is fluctuation in the two data series, but all the values are at the acceptance level for high, standard, and ultra-high resolution. For newer scanners that use a multidetector array, picture thickness is no longer a potential point of failure because it can be reconstructed from data. For the few single-slice scanners still in use, it may be valuable to verify both radiation beam width and image thickness, as the two are tied to each other, and deficiencies may occur. However, slice thickness plays a role during noise measurement; a thicker image shows a lower noise level than a thinner one.

Table-4: Collimation and corresponding nominal beam width for slice thickness measurement.

	Collimation	**Slice width mm**	**Nominal Beam width mm**	**Resolution**
Thickness 1	64x0.625	0.625	40	High
Thickness 3	40x0.625	0.625	25	High
Thickness 6	16x0.625	0.625	10	High
Thickness 9	2x0.625	0.625	1.25	High
Thickness 2	32x1.25	1.25	40	Standard
Thickness 4	12x1.25	1.25	15	Standard
Thickness 7	8x0.625	0.625	5	Standard
Thickness 8	4x0.625	0.625	2.5	Standard
Thickness 5	20x0.625	0.625	12.5	UltraHigh
Thickness 10	2x0.5	0.5	1	UltraHigh

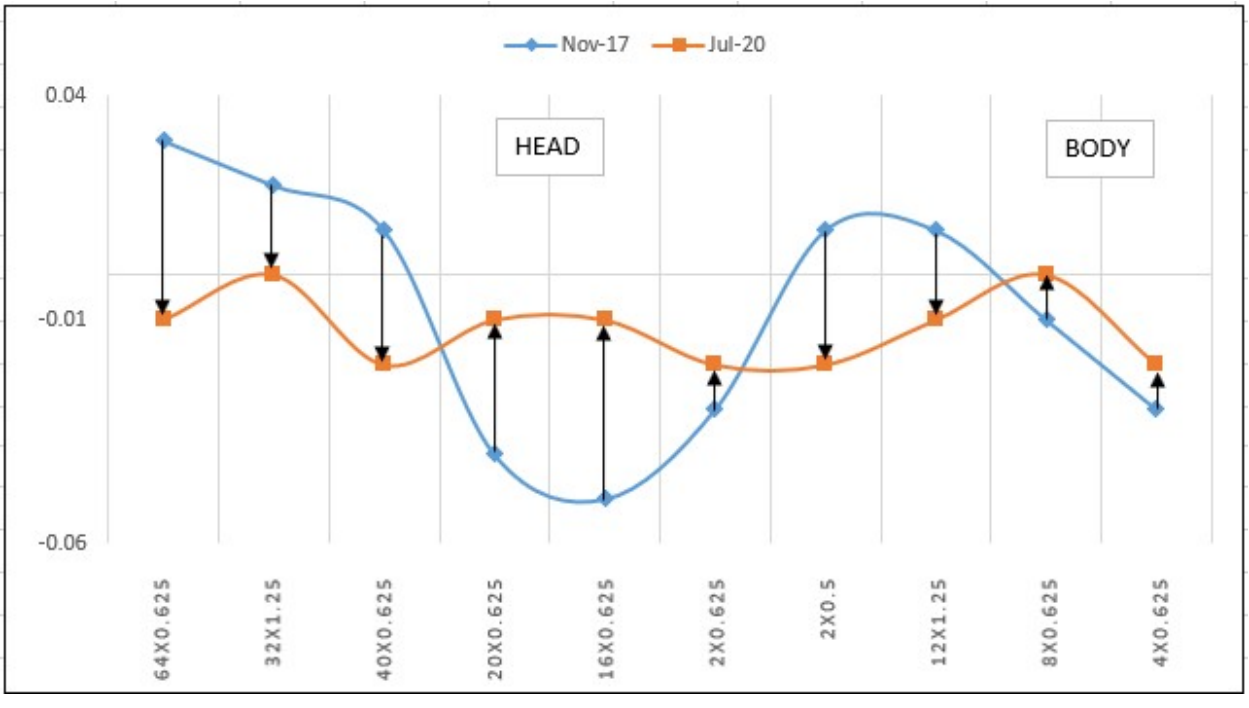

Figure-16: Slice thickness measurement at FWHM 50% for different collimation settings. Arrow indicates the direction of the change of values.

4.3 Artifacts

CT image is a mathematically reconstructed object on display that sometimes does not match physical reality. Consequently, ghost-like things in the reconstructed image have no physical existence and are known as artifacts. During the reporting period at this center, the most critical artifact reported in May 2018, which is termed a gantry artifact (Figure-17), occurred in one case. It is an eclipse-shaped, highly dense object in the images spirally repeated when the CT gantry rotates, and the patient enters through it. After several air-calibration **(Figure-18)** and long tube conditioning, we solved the artifact. Metal artifacts in several cases were recorded, where dental implants were the most common cause, and streak artifacts were noticed in the shoulder and hip regions. Overall, frequent air calibration and uniform layer (water and nylon layer) were very efficient in checking the presence of any artifact in the reconstructed images.

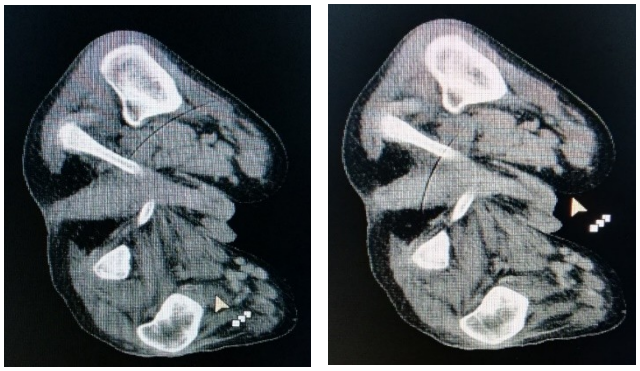

Figure-17: Gantry artifact (red arrow indicate) in CT image, Axial view.

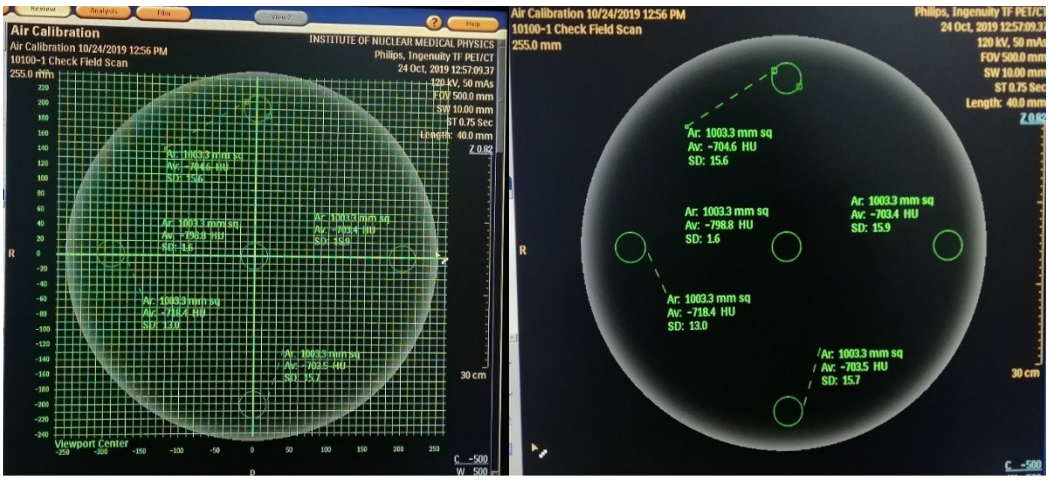

Figure-18: Air calibration: The test is done in axial mode, FOV: 500mm; Voltage:120kV; Current:67mA; mAs: 50mAs; Filter: Standard; collimation: 32X1.25mm; slice thickness:10mm; rotation time: 0.75second; Scan length: 40cm. During the scan there was no object inside the gantry as recommended by the manufacturer.

5. Conclusion

Quality assurance (QA) is critical to CT scanner operation, ensuring the system performs within acceptable limits. Traditional CT phantoms designed for single-slice scanners may be inadequate for modern helical multi-slice technology. Additionally, QC guidelines from various task groups may be outdated due to advancements in CT technology. This study focuses on the QA program for a CT scanner at a medical center in Bangladesh. The QC program followed the factory-defined protocol and utilized the vendor-provided phantom. We review the QA program requirements, including quality control parameters, tests, and testing resources, to ensure compliance with regulatory standards. While popular computerized image analysis tools like IQ Check and Constancy Test can provide valuable insights into image quality, their results may not always align perfectly with established standards. However, these tools can help identify variables within acceptable ranges, assess randomness within specific regions of the distribution curve, and monitor CT scanner performance over time. This study found that the factory-provided protocol and phantom effectively managed image quality. By adhering to these guidelines and utilizing appropriate tools, healthcare facilities can ensure the reliability and accuracy of CT imaging.

References

[1] "On a New Kind of Rays," *Nature*, vol. 53, no. 1369, pp. 274–276, Jan. 1896, doi: 10.1038/053274b0.

[2] G. N. Hounsfield, "Computerized transverse axial scanning (tomography): Part 1. Description of system," *Br. J. Radiol.*, vol. 46, no. 552, pp. 1016–1022, Dec. 1973, doi: 10.1259/0007-1285-46-552-1016.

[3] E. C. Beckmann, "CT scanning the early days," *Br. J. Radiol.*, vol. 79, no. 937, pp. 5–8, 2006, doi: 10.1259/bjr/29444122.

[4] G. N. Hounsfield, "Computed medical imaging," vol. 283, no. 1980, 2013, doi: 10.1118/1.594709.

[5] I. Isherwood, "Sir Godfrey Hounsfield," *Radiology*, vol. 234, no. 3, pp. 975–976, 2005, doi: 10.1148/radiol.2343042584.

[6] J. Ambrose, "Computerized transverse axial scanning (tomography): II. Clinical application," *Br. J. Radiol.*, vol. 46, no. 552, pp. 1023–1047, 1973, doi: 10.1259/0007-1285-46-552-1023.

[7] W. A. Kalender, W. Seissler, E. Klotz, and P. Vock, "Spiral volumetric CT with single-breath-hold technique, continuous transport, and continuous scanner rotation," *Radiology*, vol. 176, no. 1, pp. 181–183, 1990, doi: 10.1148/radiology.176.1.2353088.

[8] D. T. Ginat and R. Gupta, "Advances in Computed Tomography Imaging Technology", doi: 10.1146/annurev-bioeng-121813-113601.

[9] T. Flohr and B. Ohnesorge, "Multi-slice CT technology," *Multi-slice Dual-source CT Card. Imaging Princ. - Protoc. - Indic. - Outlook*, vol. d, pp. 41–69, 2007, doi: 10.1007/978-3-540-49546-8_3.

[10] M. Gies *et al.*, "Dose reduction in CT by anatomically adapted tube current modulation," vol. 2235, no. 1999, 2013, doi: 10.1118/1.598779.

[11] W. A. Kalender, H. Wolf, C. Suess, W. A. Kalender, H. Wolf, and C. Suess, "Dose reduction in CT by anatomically adapted tube current modulation . II . Phantom

measurements," vol. 2248, no. 1999, 2012, doi: 10.1118/1.598738.
[12] T. Fuchs, M. Kachelrieß, and W. A. Kalender, "Technical advances in multi–slice spiral CT," *Eur. J. Radiol.*, vol. 36, no. 2, pp. 69–73, Nov. 2000, doi: 10.1016/S0720-048X(00)00269-2.
[13] I. Ilias, A. Sahdev, R. H. Reznek, A. B. Grossman, and K. Pacak, "The optimal imaging of adrenal tumours: A comparison of different methods," *Endocr. Relat. Cancer*, vol. 14, no. 3, pp. 587–599, 2007, doi: 10.1677/ERC-07-0045.
[14] F. Zarb, L. Rainford, and M. F. McEntee, "Image quality assessment tools for optimization of CT images," *Radiography*, vol. 16, no. 2, pp. 147–153, 2010, doi: 10.1016/j.radi.2009.10.002.
[15] F. R. Verdun *et al.*, "Image quality in CT: From physical measurements to model observers," *Phys. Medica*, vol. 31, no. 8, pp. 823–843, 2015, doi: 10.1016/j.ejmp.2015.08.007.
[16] F. van Ommen *et al.*, "Image quality of conventional images of dual-layer SPECTRAL CT: A phantom study," *Med. Phys.*, vol. 45, no. 7, pp. 3031–3042, 2018, doi: 10.1002/mp.12959.
[17] O. Rampado *et al.*, "Effective dose and image quality evaluations of an automatic CT tube current modulation system with an anthropomorphic phantom," *Eur. J. Radiol.*, vol. 72, no. 1, pp. 181–187, 2009, doi: 10.1016/j.ejrad.2008.06.027.
[18] T. Torfeh, S. Beaumont, J. P. Guédon, and E. Denis, "Evaluation of two software tools dedicated to an automatic analysis of the CT scanner image spatial resolution," *Annu. Int. Conf. IEEE Eng. Med. Biol. - Proc.*, pp. 3910–3913, 2007, doi: 10.1109/IEMBS.2007.4353188.
[19] K. Gulliksrud, C. Stokke, and A. C. Trægde Martinsen, "How to measure CT image quality: Variations in CT-numbers, uniformity and low contrast resolution for a CT quality assurance phantom," *Phys. Medica*, vol. 30, no. 4, pp. 521–526, 2014, doi: 10.1016/j.ejmp.2014.01.006.
[20] E. Commission, "European guidelines on quality criteria for computed tomography," *EU Publ.*, vol. CG-NA-16-2, 2000, [Online]. Available: https://op.europa.eu/en/publication-detail/-/publication/d229c9e1-a967-49de-b169-59ee68605f1a
[21] IAEA, "Report. No 19: Quality Assurance for Computed Tomography - Diagnostic and Therapy Applications," 2012.
[22] S. Mutic *et al.*, "Quality assurance for computed-tomography simulators and the computed-tomography-simulation process: Report of the AAPM Radiation Therapy Committee Task Group No. 66," *Med. Phys.*, vol. 30, no. 10, pp. 2762–2792, 2003, doi: 10.1118/1.1609271.
[23] C. Dillon *et al.*, "ACR 2017 Computed Tomography Quality Control manual," 2017.
[24] L. Rothenberg, "Quality Control in CT," *AAPM Montr. Conf.*, pp. 1–3, 2002.
[25] EC, *European Comission, Radiation Protection nº162, Criteria for Acceptability of Medical Radiological equipment used in diagnostica radiology, nuclear medicine and radiotherapy*. 2012. doi: 10.2768/22561.
[26] K. A. Jessen *et al.*, "Quality Criteria Development within the Fourth Framework Research Programme: Computed Tomography," *Radiat. Prot. Dosimetry*, vol. 90, no. 1, pp. 79–83, Aug. 2000, doi: 10.1093/oxfordjournals.rpd.a033147.
[27] College of Physicians and Surgeons of British Columbia, "Radiology and CT Quality Control Procedures Workbook," pp. 1–134, 2018.
[28] C. Steiding, D. Kolditz, and W. A. Kalender, "A quality assurance framework for the fully automated and objective evaluation of image quality in cone-beam computed

tomography," *Med. Phys.*, vol. 41, no. 3, 2014, doi: 10.1118/1.4863507.
[29] Z. Mansour, A. Mokhtar, A. Sarhan, M. T. Ahmed, and T. El-Diasty, "Quality control of CT image using American College of Radiology (ACR) phantom," *Egypt. J. Radiol. Nucl. Med.*, vol. 47, no. 4, pp. 1665–1671, 2016, doi: 10.1016/j.ejrnm.2016.08.016.
[30] IEC, "IEC 61223-3-5:2019: Evaluation and routine testing in medical imaging departments - Part 3-5: Acceptance and constancy tests - Imaging performance of computed tomography X-ray equipment," 2019. [Online]. Available: https://webstore.iec.ch/publication/59789
[31] J. M. Boone *et al.*, "ICRU Report No. 87: Radiation dose and image-quality assessment in computed tomography," *J. ICRU*, vol. 12, no. 1, pp. 9–149, 2012, doi: 10.1093/jicru.
[32] M. H. McKetty, "The AAPM/RSNA Physics Tutorial for Residents: X-ray Attenuation," *Radiographics*, vol. 18, no. 1, pp. 151–163, 1998, doi: 10.1148/radiographics.18.1.9460114.
[33] M. E. Phelps, E. J. Hoffman, and M. M. Ter Pogossian, "Attenuation coefficients of various body tissues, fluids, and lesions at photon energies of 18 to 136 keV," *Radiology*, vol. 117, no. 3 I, pp. 573–583, 1975, doi: 10.1148/117.3.573.
[34] W. R. Hendee, E. R. Ritenour, and K. R. Hoffmann, *Medical Imaging Physics, Fourth Edition*, vol. 30, no. 4. 2003. doi: 10.1118/1.1563664.
[35] S. Rosslyn, "Digital Imaging and Communications in Medicine (DICOM) Part 14 : Grayscale Standard Display Function," 2011.
[36] J. A. Bryant, N. A. Drage, and S. Richmond, "CT number definition," *Radiat. Phys. Chem.*, vol. 81, no. 4, pp. 358–361, 2012, doi: 10.1016/j.radphyschem.2011.12.026.
[37] I. J. Glide-Hurst, C., Chen, D., Zhong, H., & Chetty, "Changes realized from extended bit-depth and metal artifact reduction in CT," vol. 48202, no. May, pp. 1–10, 2013, doi: 10.1118/1.4805102.
[38] A. P. Richard Bibb, Dominic Eggbeer, "Medical Modelling," in *Medical Modelling*, 2nd ed., Elsevier, 2015, pp. 7–34. doi: https://doi.org/10.1016/B978-1-78242-300-3.00002-0.
[39] M. O. Lagravère, Y. Fang, J. Carey, R. W. Toogood, G. V. Packota, and P. W. Major, "Density conversion factor determined using a cone-beam computed tomography unit NewTom QR-DVT 9000," *Dentomaxillofacial Radiol.*, vol. 35, no. 6, pp. 407–409, 2006, doi: 10.1259/dmfr/55276404.
[40] M. J. da S. Campos, "Bone mineral density in cone beam computed tomography: Only a few shades of gray," *World J. Radiol.*, vol. 6, no. 8, p. 607, 2014, doi: 10.4329/wjr.v6.i8.607.
[41] Philips, *CT System Operation Manuaal*.
[42] "International Electrotecnical Commission IEC 61223-3-5. Evaluation and Routine Testing in Medical Imaging Departments – part 3– 5: Acceptance Tests – Imaging Performance of Computed Tomography X-ray Equipment (2013)".
[43] W. R. Reddingerddinger, *CT Image Quality*. 1998.
[44] ICRU 44, "ICRU Report 44: Tissue Substitutes in Radiation Dosimetry and Measurements," *ICRU Publ.*, vol. os 23, no. 1, 1989.
[45] CIRS, "IMRT Thorax Phantom: Data Sheet."
[46] Task_Group-2, "AAPM report No. 39: Specification and Acceptance Testing of Computed Tomography Scanners," 1993.
[47] C. H. McCollough *et al.*, "The phantom portion of the American College of Radiology (ACR) Computed Tomography (CT) accreditation program: Practical tips, artifact examples, and pitfalls to avoid," *Med. Phys.*, vol. 31, no. 9, pp. 2423–2442, 2004, doi: 10.1118/1.1769632.

[48] C. H. McCollough *et al.*, "Degradation of CT low-contrast spatial resolution due to the use of iterative reconstruction and reduced dose levels," *Radiology*, vol. 276, no. 2, pp. 499–506, 2015, doi: 10.1148/radiol.15142047.
[49] M. E. Baker *et al.*, "Contrast-to-noise ratio and low-contrast object resolution on full- and low-dose MDCT: Safire versus filtered back projection in a low-contrast object phantom and in the liver," *Am. J. Roentgenol.*, vol. 199, no. 1, pp. 8–18, 2012, doi: 10.2214/AJR.11.7421.
[50] J. M. Kofler *et al.*, "Assessment of Low-Contrast Resolution for the American College of Radiology Computed Tomographic Accreditation Program: What Is the Impact of Iterative Reconstruction?," *J. Comput. Assist. Tomogr.*, vol. 39, no. 4, pp. 619–623, 2015, doi: 10.1097/RCT.0000000000000245.
[51] D. Racine, A. H. Ba, J. G. Ott, F. O. Bochud, and F. R. Verdun, "Objective assessment of low contrast detectability in computed tomography with Channelized Hotelling Observer," *Phys. Medica*, vol. 32, no. 1, pp. 76–83, 2016, doi: 10.1016/j.ejmp.2015.09.011.
[52] D. J. Goodenough and K. E. Weaver, "Factors related to low contrast resolution in CT scanners," *Comput. Radiol.*, vol. 8, no. 5, pp. 297–308, 1984, doi: 10.1016/0730-4862(84)90042-8.
[53] D. J. Goodenough, "Catphan 500 and 600 Manual," *Phantom Lab.*, vol. 1, no. 1, pp. 1–33, 2006.
[54] J. E. Barnes, "Characteristics and control of contrast in CT.," *Radiographics*, vol. 12, no. 4, pp. 825–837, 1992, doi: 10.1148/radiographics.12.4.1636042.
[55] S. K. N. Dilger *et al.*, localization of liver lesions in abdominal CT imaging: I. Correlation of human observer performance between anatomical and uniform backgrounds," *Phys. Med. Biol.*, vol. 64, no. 10, May 2019, doi: 10.1088/1361-6560/ab1a45.
[56] D. Kirkaldie, "GE CT QA Phantom." https://help.imageowl.com/hc/en-us/articles/4403105543187-GE-CT-QA-Phantom
[57] AAPM, "AAPM Report No. 1: Phantoms for Performance Evaluation and Quality Assurance of CT Scanners," 1977. [Online]. Available: http://www.aapm.org/pubs/reports/rpt_01.pdf
[58] G. Acri, M. G. Tripepi, F. Causa, B. Testagrossa, R. Novario, and G. Vermiglio, "Slice-thickness evaluation in CT and MRI: an alternative computerised procedure," *Radiol. Medica*, vol. 117, no. 3, pp. 507–518, 2012, doi: 10.1007/s11547-011-0775-5.
[59] ACR, "Computed Tomography (CT) Accreditation Program : PHANTOM TESTING INSTRUCTIONS," 1891.
[60] L. Safety, E. Safety, A. Safety, A. Safety, E. Accuracy, and M. Performance, "CT Scanner Acceptance Testing - ImPACT," *Inf. Leafl.*, no. 1, pp. 1–8, 2001.
[61] Sun_Nuclear_Corporation, "CT ACR 464 Phantom," 2020. [Online]. Available: https://www.sunnuclear.com/products/ct-acr-464-phantom
[62] C. J. Bischof and J. C. Ehrhardt, "Modulation transfer function of the EMI CT head scanner," vol. 163, no. 1977, 2012, doi: 10.1118/1.594305.
[63] D. Radiology, "One-year analysis of Elekta CBCT image quality using NPS and MTF," vol. 17, no. 3, pp. 211–222, 2016.
[64] A. Workman and D. S. Brettle, "Physical performance measures of radiographic imaging systems.," *Dentomaxillofac. Radiol.*, vol. 26, no. 3, pp. 139–146, 1997, doi: 10.1038/sj.dmfr.4600241.
[65] S. Punwani, J. Zhang, W. Davies, R. Greenhalgh, and P. Humphries, "Paediatric CT: the effects of increasing image noise on pulmonary nodule detection," *Pediatr. Radiol.*, vol. 38, no. 2, pp. 192–201, Feb. 2008, doi: 10.1007/s00247-007-0694-8.

[66] AAPM, “AAPM CT Performance Phantom,” pp. 1–2.
[67] “Catphan 600 Series.” https://www.phantomlab.com/catphan-600
[68] M. Diwakar and M. Kumar, “A review on CT image noise and its denoising,” *Biomed. Signal Process. Control*, vol. 42, pp. 73–88, 2018, doi: 10.1016/j.bspc.2018.01.010.
[69] B. Chen, O. Christianson, J. M. Wilson, and E. Samei, “Assessment of volumetric noise and resolution performance for linear and nonlinear CT reconstruction methods,” *Med. Phys.*, vol. 41, no. 7, 2014, doi: 10.1118/1.4881519.
[70] IPEM, “Report 91 : Recommended Standards for the Routine Performance Testing of Diagnostic X-Ray Systems,” 2010.
[71] S. Mutic *et al.*, “Quality assurance for computed-tomography simulators and the computed- tomography-simulation process : Report of the AAPM Radiation Therapy Committee Task Group No . 66 Quality assurance for computed-tomography simulators and the computed- tomography-simu,” vol. 1773, no. 66, 2014, doi: 10.1118/1.1609271.
[72] D. P. Chakraborty, “ROC curves predicted by a model of visual search,” *Phys. Med. Biol.*, vol. 51, no. 14, pp. 3463–3482, Jul. 2006, doi: 10.1088/0031-9155/51/14/013.
[73] P. Jerrold T. Bushberg, PhD; J. Anthony Seibert, PhD; Edwin M. Leidholdt, Jr., PhD; John M. Boone, *The Essential Physics of Medical Imaging*, 2nd ed. 2003.